12. N. Zwahlen et al., Astron. Astrophys. **425**, L45–L48 (2004).
13. V. K. Narayanan, A. Gould, Astrophys. J. **523**, 328–339 (1999).
14. V. V. Makarov, Astron. J. **124**, 3299–3304 (2002).
15. M. A. C. Perryman et al., Astron. Astrophys. **369**, 339–363 (2001).
16. L. Loinard et al., Astrophys. J. **671**, 546–554 (2007).
17. E. Høg et al., Astron. Astrophys. **355**, L27–L30 (2000).
18. N. Zacharias et al., Astron. J. **145**, 44 (2013).
19. S. M. Percival, M. Salaris, M. A. T. Groenewegen, Astron. Astrophys. **429**, 887–894 (2005).
20. D. Stello, P. E. Nissen, Astron. Astrophys. **374**, 105–115 (2001).
21. M. A. Giannuzzi, Astron. Astrophys. **293**, 360 (1995).
22. F. van Leeuwen, The Pleiades, an astrometric and photometric study of an open cluster. Thesis, Leiden University, Leiden, Netherlands (1983).
23. B. Nicolet, Astron. Astrophys. **104**, 185 (1981).
24. J. Southworth, P. F. L. Maxted, B. Smalley, Astron. Astrophys. **429**, 645–655 (2005).
25. U. Munari et al., Astron. Astrophys. **418**, L31–L34 (2004).
26. X. Pan, M. Shao, S. R. Kulkarni, Nature **427**, 326–328 (2004).
27. S. Röser, E. Schilbach, A new assessment of the kinematic distance to the Pleiades: based on radial velocities and proper motions only, Proc. IAU Symp. **289**, 66 (2013).

CIRCUMSTELLAR DISKS

Large impacts around a solar-analog star in the era of terrestrial planet formation

Huan Y. A. Meng,[1] Kate Y. L. Su,[2] George H. Rieke,[1,2] David J. Stevenson,[3] Peter Plavchan,[4,5] Wiphu Rujopakarn,[2,6,7] Carey M. Lisse,[8] Saran Poshyachinda,[9] Daniel E. Reichart[10]

The final assembly of terrestrial planets occurs via massive collisions, which can launch copious clouds of dust that are warmed by the star and glow in the infrared. We report the real-time detection of a debris-producing impact in the terrestrial planet zone around a 35-million-year-old solar-analog star. We observed a substantial brightening of the debris disk at a wavelength of 3 to 5 micrometers, followed by a decay over a year, with quasi-periodic modulations of the disk flux. The behavior is consistent with the occurrence of a violent impact that produced vapor out of which a thick cloud of silicate spherules condensed that were then ground into dust by collisions. These results demonstrate how the time domain can become a new dimension for the study of terrestrial planet formation.

Circumstellar disks are where planetary systems form and evolve. Gas-rich and optically thick protoplanetary disks are born together with young stars but dissipate within a few million years (My), setting the time scale for gas-giant planet formation (1). Dusty, optically thin debris disks then emerge, sustained by the fragmentation of colliding planetesimals (2). They are warmed by their stars and light up in the infrared (IR), allowing them to be detected over the entire lifetimes of main-sequence stars. Consequently, debris disks are ideal tools in which to search for phases occurring in other planetary systems that are analogous to major events in the evolution of the solar system, such as the formation of terrestrial planets. Dynamical simulations and meteoritics indicate that the end stage of terrestrial planet formation, from ~30 to ~100 My (3, 4), is marked by frequent large impacts, up to the scale of the one leading to the formation of the Moon (5–7). Such events can produce a huge amount of dust, which may dramatically increase the IR emission from the debris disk (8).

ID8 (2MASS J08090250-4858172) is a young solar-analog star, with spectral type G6V and solar metallicity, in the 35-My-old open star cluster NGC 2547 (9). It emits strongly in the IR, with a fractional disk luminosity of $L_{disk}/L_* = 3.2 \times 10^{-2}$ (L_*, stellar luminosity) (10). The mid-IR spectrum of ID8 (observed in 2007) shows strong crystalline silicate features between 8 and 30 μm, indicative of very fine dust particles (Fig. 1); models of the observed spectral energy distribution (SED) require submicrometer-sized amorphous silicate dust particles as well (10). Particles are blown out by radiation pressure and are lost to the system if the ratio of radiation to gravitational forces is larger than 0.5. For ID8, the critical radius (11) below which nonporous silicate grains are lost is ~0.5 μm. The tiniest particles in the disk are smaller than this limit, suggesting ongoing dust replenishment in the system.

The disk emission was recently found to vary on a yearly time scale (8). Collisional cascades among planetesimals sustain most debris disks. However, variations this rapid cannot be sup-

ported by this means, because the cascade time scales for significant variations in dust production are at least a few hundred orbits (8). To explore the origin of the variations, we have used the Infrared Array Camera [IRAC (12)] onboard the Spitzer Space Telescope to monitor the ID8 system. The observations extended from 25 May 2012 to 23 August 2013, providing a total time baseline of 454 days, with a 157-day gap between visibility windows. At the same time, intensive optical monitoring of ID8 was obtained from the ground in the V and Cousins I bands, where we found that the output of the star is stable within ~1.5% root mean square (supplementary text).

Because the stellar contribution is effectively constant in time, we fitted its spectrum and removed it from the total (star + disk) IR fluxes to obtain the light curves of the debris disk, as shown in Fig. 2. This revealed an average disk color of [3.6] − [4.5] = 1.00, corresponding to a blackbody temperature of 730 K, which is consistent with the temperatures found in previous analyses of the mid-IR spectroscopy (10). We calculated the expected color trend of the entire ID8 system for possible causes of the disk variations and compared it with our data. The result is not conclusive within the errors, but suggests that a combination of changing dust temperature and dust-emitting

[1]Lunar and Planetary Laboratory and Department of Planetary Sciences, University of Arizona, 1629 East University Boulevard, Tucson, AZ 85721, USA. [2]Steward Observatory and Department of Astronomy, University of Arizona, 933 North Cherry Avenue, Tucson, AZ 85721, USA. [3]Division of Geological and Planetary Sciences, California Institute of Technology, MC 170-25, 1200 East California Boulevard, Pasadena, CA 91125, USA. [4]NASA Exoplanet Science Institute, California Institute of Technology, MC 100-22, 770 South Wilson Avenue, Pasadena, CA 91125, USA. [5]Missouri State University, 901 South National Avenue, Springfield, MO 65897, USA. [6]Department of Physics, Faculty of Science, Chulalongkorn University, 254 Phayathai Road, Pathumwan, Bangkok 10330, Thailand. [7]Kavli Institute for the Physics and Mathematics of the Universe (WPI), Todai Institute for Advanced Study, University of Tokyo, 5-1-5 Kashiwanoha, Kashiwa, 277-8583, Japan. [8]Space Department, Applied Physics Laboratory, Johns Hopkins University, 11100 Johns Hopkins Road, Laurel, MD 20723, USA. [9]National Astronomical Research Institute of Thailand (Public Organization), Ministry of Science and Technology, 191 Siriphanich Building, Huay Kaew Road, Muang District, Chiang Mai 50200, Thailand. [10]Department of Physics and Astronomy, Campus Box 3255, University of North Carolina at Chapel Hill, Chapel Hill, NC 27599, USA.

area, or in area alone rather than purely in temperature, may be responsible for the disk variations (supplementary text).

In the following analysis, we focus on the 4.5-μm data where we have observations from both years, and the disk is measured at a higher signal-to-noise ratio. The data at 3.6 μm show consistent behavior, although at lower signal-to-noise ratio. In 2012, the disk flux density stayed

Fig. 1. Spectrum of the ID8 system. The photometric errors are smaller than the symbol size and are not shown; errors of the Spitzer/IRS spectrum are indicated as vertical lines. Red crosses at 24 μm show the three epochs of Spitzer/MIPS observations that led to the discovery of disk variability (8). The ranges of the new measurements at 3.6 and 4.5 μm in this work are plotted as blue vertical lines. CTIO, Cerro Tololo Inter-American Observatory; 2MASS, 2 Micron All Sky Survey; MIPS, Multiband Imaging Photometer for Spitzer; IRS, Infrared Spectrograph; WISE, Wide-field Infrared Survey Explorer.
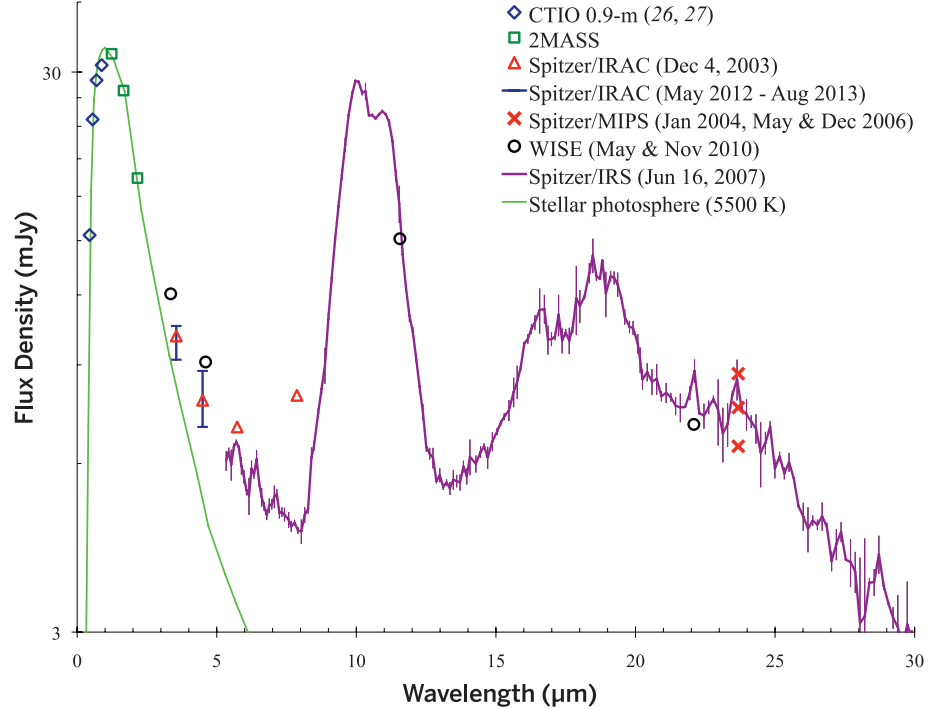

◇ CTIO 0.9-m (26, 27)
□ 2MASS
△ Spitzer/IRAC (Dec 4, 2003)
— Spitzer/IRAC (May 2012 - Aug 2013)
✕ Spitzer/MIPS (Jan 2004, May & Dec 2006)
○ WISE (May & Nov 2010)
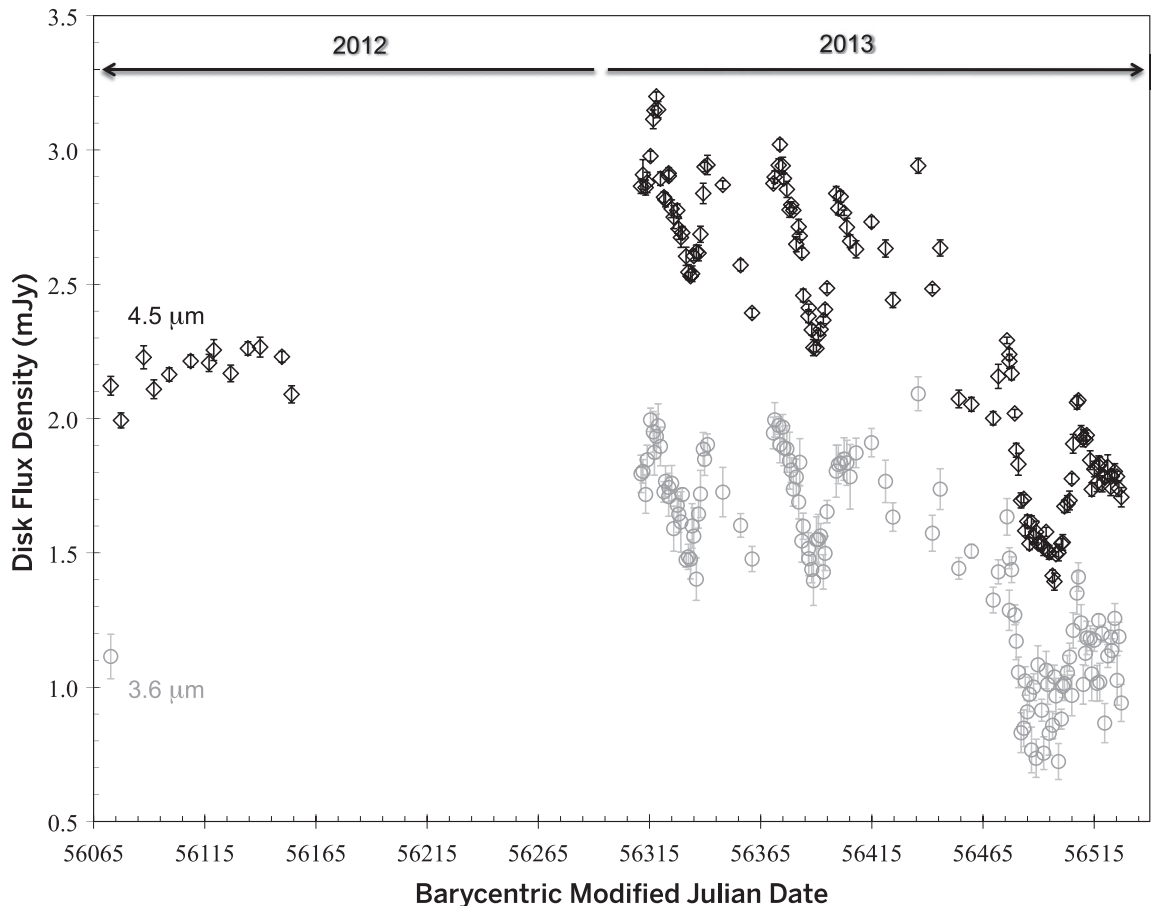— Spitzer/IRS (Jun 16, 2007)
— Stellar photosphere (5500 K)

Fig. 2. Light curves of the debris disk of ID8 at 3.6 and 4.5 μm, assuming no error in photosphere subtraction. The gap between Barycentric Modified Julian Date (BMJD) 56155 and 56311 occurred when ID8 was outside of the Spitzer visibility windows.

near 2.2 milli-Jansky (mJy), despite ~10% variations. However, at the start of 2013 it had brightened to above 3.0 mJy, indicating a significant increase in the amount of dust, probably from a new impact before 2013. This elevated level then decayed throughout 2013. An exponential fit suggests a decay time scale of ~370 days at both wavelengths. This is too fast to be reconciled with decades-long collisional cascades (8) and is too slow for the direct radiative blowout of tiny particles, which should take <30 days at the orbit derived below for the disk.

To better understand the impact, we estimate the disk mass based on a fit to the entire mid-IR spectrum, which is dominated by small grains. Because the new debris in the disk has not reached equilibrium in a full collisional cascade, we could not make the conventional assumption of a power-law size distribution. For emitting grains of 0.5 μm in radius, we found a disk mass of 1.1×10^{19} kg, which is a lower limit because it ignores larger particles. An independent estimate assuming a power-law grain size distribution up to 1 mm obtains an identical mass estimate (10). This mass, if the grains were compacted into a solid body, is equivalent to an ~180-km-diameter asteroid (of density 3700 kg m^{-3}). Given the estimated mass and particle size, the ID8 disk may be optically thick, in which significant mass could be obscured and unseen.

Considering the decay in 2013, and assuming it applies to the full spectrum, we estimated the mass loss rate to be at least 10^{11} kg s^{-1}. The spectrum was obtained in 2007; however, the Spitzer and WISE photometric points (Fig. 1) imply that the mid-IR spectrum had a similar shape at least from January 2004 through November 2010. That is, it appears that the small grains, with a net volume of an ~180-km-diameter asteroid, were lost from the system and would have to be replenished on a decadal (or shorter) time scale to maintain the mid-IR spectrum. Though arising from different physical processes, the mass loss rate is five to seven orders of magnitude greater than the dust mass loss rates of comets Hale-Bopp (13) and Halley (14), which are among the dustiest comets known in the solar system, and is three orders of magnitude greater than that of the evaporating planet KIC 12557548b (15).

The variability of the IR emission of ID8 is much too fast to arise in a conventional debris disk sustained by a collisional cascade (8). We hypothesize that the impact responsible for the increased disk emission in 2013 involved two large bodies and was sufficiently violent to yield a silica-rich vapor plume. Glassy silicate spherules will condense from the vapor with diverse forms (16), consistent with the presence of amorphous silicates in the SED model (10). In this case, there may have been temporal spectral features after the new impact, but they would have been missed because we do not have a new mid-IR spectrum in 2013. The condensation process has been modeled in (17), which shows that the typical spherule size depends sensitively on the circumstances of the impact, particularly its velocity, but ranges from about 10 μm to 1 mm. The condensates are produced quickly over several hours. Initially, the cloud of spherules will not radiate efficiently in the mid-IR, because the total surface area of all the spherules is small. However, they will break each other down through collisions, which generate the observed micrometer-sized or smaller particles as daughter products. The IR output will rise as the mass is distributed into many small grains, making the consequences of the initial impact visible as an increase in the IR emission.

Because the size distribution of condensate spherules is strongly peaked around the average (17), we treat them as being equal in size. Then a rough estimate of the time scale for destroying them (and hence for the decay of the debris cloud) can be obtained by attributing all the disk mass to them immediately after the impact and assuming that they are removed by breakdown in a collisional cascade with eventual ejection, when their daughter particles are submicrometer in size, by radiation pressure. We found that different models for the destruction rate of such spherules give consistent time scales (18, 19). To order of magnitude, the range of decay time scales as a function of spherule size from 10 to 1000 μm is 100 days to 10 years. The observed decay time of the ID8 disk corresponds to a spherule size of ~100 μm, which corresponds to an impact velocity of 15 to 18 km s^{-1} [for a body with a diameter of 100 to 1000 km impacting on an even larger one (17)]. Thus, the 1-year exponential decay time scale is a natural result for a system where seed grains have condensed from a vapor cloud and are destroying themselves through
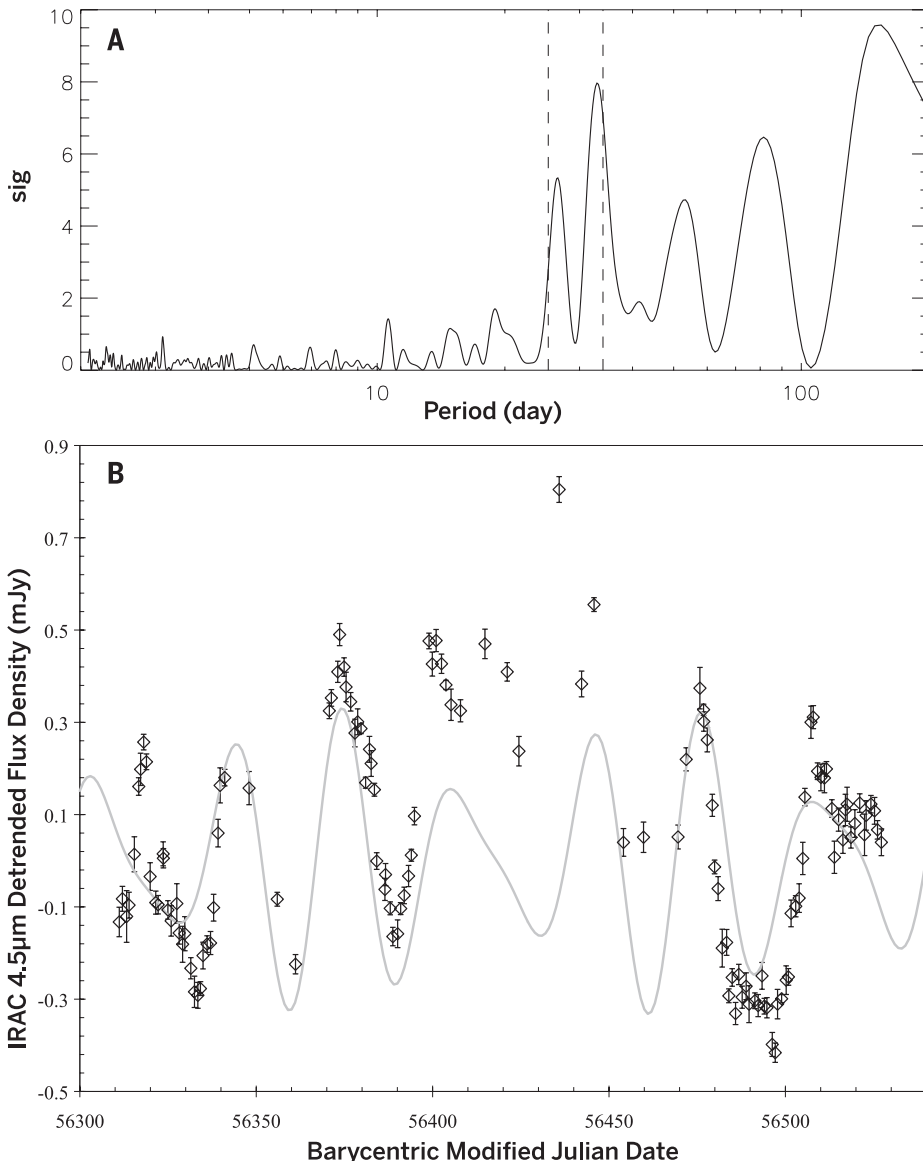

Fig. 3. Analysis of the 4.5-μm time series of the ID8 disk. (**A**) **Periodogram of the detrended 2013 light curve.** The vertical dashed lines represent the identified periods P_1 and P_2, which are determined after removing the strongest frequency in each iteration (22) and thus appear slightly offset from the raw peak positions. (**B**) Detrended 4.5-μm data (black diamonds) with the composite of two sine waves of P_1 and P_2 (gray curve). Because their real waveforms are probably nonsinusoidal, the comparison is meaningful only for the general timing of the highs and lows.

collisions. An analysis with some similarities to ours for the bright debris disk of HD 172555 (20) found that dust created in a hypervelocity impact will have a size slope of ~ –4, in agreement with the fits of (10) to the IR spectrum of ID8.

After the exponential decay is removed from the data ("detrending"), the light curves at both wavelengths appear to be quasi-periodic. The regular recovery of the disk flux and lack of extraordinary stellar activity essentially eliminate coronal mass ejection (21) as a possible driver of the disk variability. We employed the SigSpec algorithm (22) to search for complex patterns in the detrended, post-impact 2013 light curve. The analysis identified two significant frequencies with comparable amplitudes, whose periods are $P_1 = 25.4 \pm 1.1$ days and $P_2 = 34.0 \pm 1.5$ days (Fig. 3A) and are sufficient to qualitatively reproduce most of the observed light curve features (Fig. 3B). The quoted uncertainties (23) do not account for systematic effects due to the detrending and thus are lower limits to the real errors. Other peaks with longer periods in the periodogram are aliases or possibly reflect long-term deviation from the exponential decay. These artifacts make it difficult to determine whether there are weak real signals near those frequencies.

We now describe the most plausible interpretation of this light curve that we have found. The two identified periods have a peak-to-peak amplitude of ~6×10^{-3} in fractional luminosity, which provides a critical constraint for models of the ID8 disk. In terms of sky coverage at the disk distance inferred from the IR SED, such an amplitude requires the disappearance and reappearance every ~30 days of the equivalent of an opaque, stellar-facing "dust panel" of radius ~110 Jupiter radii. One possibility is that the disk flux periodicity arises from recurring geometry that changes the amount of dust that we can see. At the time of the impact, fragments get a range of kick velocities when escaping into interplanetary space. This will cause Keplerian shear of the cloud (24), leading to an expanding debris concentration along the original orbit (supplementary text). If the ID8 planetary system is roughly edge-on, the longest dimension of the concentration will be parallel to our line of sight at the greatest elongations and orthogonal to the line of sight near conjunctions to the star. This would cause the optical depth of the debris to vary within an orbital period, in a range on the order of 1 to 10 according to the estimated disk mass and particle sizes. Our numerical simulations of such dust concentrations on moderately eccentric orbits are able to produce periodic light curves with strong overtones. P_2 and P_1 should have a 3:2 ratio if they are the first- and second-order overtones of a fundamental, which is consistent with the measurements within the expected larger errors (<2σ or better). In this case, the genuine period should be 70.8 ± 5.2 days (lower-limit errors), a value where it may have been submerged in the periodogram artifacts. This period corresponds to a semimajor axis of ~0.33 astronomical units, which is consistent with the temperature and distance suggested by the spectral models (10).

Despite the peculiarities of ID8, it is not a unique system. In 2012 and 2013, we monitored four other "extreme debris disks" (with disk fractional luminosity $\geq 10^{-2}$) around solar-like stars with ages of 10 to 120 My. Various degrees of IR variations were detected in all of them. The specific characteristics of ID8 in the time domain, including the yearly exponential decay, additional more rapid weekly to monthly changes, and color variations, are also seen in other systems. This opens up the time domain as a new dimension for the study of terrestrial planet formation and collisions outside the solar system. The variability of many extreme debris disks in the era of the final buildup of terrestrial planets may provide new possibilities for understanding the early solar system and the formation of habitable planets (25).

REFERENCES AND NOTES

1. R. Helled et al., in Protostars and Planets VI, H. Beuther, R. Klessen, C. Dullemond, T. Henning, Eds. (Univ. of Arizona Press, Tucson, AZ, 2014), in press; available at http://arxiv.org/abs/1311.1142.
2. M. C. Wyatt, Annu. Rev. Astron. Astrophys. 46, 339–383 (2008).
3. K. Righter, D. P. O'Brien, Proc. Natl. Acad. Sci. U.S.A. 108, 19165–19170 (2011).
4. S. N. Raymond, E. Kokubo, A. Morbidelli, R. Morishima, K. J. Walsh, in Protostars and Planets VI, H. Beuther, R. Klessen, C. Dullemond, T. Henning, Eds. (Univ. of Arizona Press, Tucson, AZ, 2014), in press; available at http://arxiv.org/abs/1312.1689.
5. R. M. Canup, Annu. Rev. Astron. Astrophys. 42, 441–475 (2004).
6. M. Ćuk, S. T. Stewart, Science 338, 1047–1052 (2012).
7. R. M. Canup, Science 338, 1052–1055 (2012).
8. H. Y. A. Meng et al., Astrophys. J. 751, L17–L21 (2012).
9. D. R. Soderblom, L. A. Hillenbrand, R. D. Jeffries, E. E. Mamajek, T. Naylor, in Protostars and Planets VI, H. Beuther, R. Klessen, C. Dullemond, T. Henning, Eds. (Univ. of Arizona Press, Tucson, AZ, 2014), in press; available at http://arxiv.org/abs/1311.7024.
10. J. Olofsson et al., Astron. Astrophys. 542, 90–115 (2012).
11. P. Artymowicz, Astrophys. J. 335, L79–L82 (1988).
12. G. G. Fazio et al., Astrophys. J. Suppl. Ser. 154, 10–17 (2004).
13. D. Jewitt, H. Matthews, Astron. J. 117, 1056–1062 (1999).
14. J. A. M. McDonnell et al., Nature 321, 338–341 (1986).
15. D. Perez-Becker, E. Chiang, Mon. Not. R. Astron. Soc. 433, 2294–2309 (2013).
16. P. H. Warren, Geochim. Cosmochim. Acta 72, 3562–3585 (2008).
17. B. C. Johnson, H. J. Melosh, Icarus 217, 416–430 (2012).
18. M. C. Wyatt, W. R. F. Dent, Mon. Not. R. Astron. Soc. 334, 589–607 (2002).
19. B. Zuckerman, I. Song, Astrophys. J. 758, 77–86 (2012).
20. B. C. Johnson et al., Astrophys. J. 761, 45–57 (2012).
21. R. Osten et al., Astrophys. J. 765, L44–L46 (2013).
22. P. Reegen, Astron. Astrophys. 467, 1353–1371 (2007).
23. T. Kallinger, P. Reegen, W. W. Weiss, Astron. Astrophys. 481, 571–574 (2008).
24. S. J. Kenyon, B. C. Bromley, Astron. J. 130, 269–279 (2005).
25. S. Elser, B. Moore, J. Stadel, R. Morishima, Icarus 214, 357–365 (2011).
26. T. Naylor et al., Mon. Not. R. Astron. Soc. 335, 291–310 (2002).
27. R. D. Jeffries, T. Naylor, C. R. Devey, E. J. Totten, Mon. Not. R. Astron. Soc. 351, 1401–1422 (2004).

SUPERFLUIDITY

A mixture of Bose and Fermi superfluids

I. Ferrier-Barbut,* M. Delehaye, S. Laurent, A. T. Grier,† M. Pierce, B. S. Rem,‡ F. Chevy, C. Salomon

Superconductivity and superfluidity of fermionic and bosonic systems are remarkable many-body quantum phenomena. In liquid helium and dilute gases, Bose and Fermi superfluidity has been observed separately, but producing a mixture in which both the fermionic and the bosonic components are superfluid is challenging. Here we report on the observation of such a mixture with dilute gases of two lithium isotopes, lithium-6 and lithium-7. We probe the collective dynamics of this system by exciting center-of-mass oscillations that exhibit extremely low damping below a certain critical velocity. Using high-precision spectroscopy of these modes, we observe coherent energy exchange and measure the coupling between the two superfluids. Our observations can be captured theoretically using a sum-rule approach that we interpret in terms of two coupled oscillators.

In recent years, ultracold atoms have emerged as a unique tool to engineer and study quantum many-body systems. Examples include weakly interacting Bose-Einstein condensates (1, 2), two-dimensional gases (3), and the superfluid-Mott insulator transition (4) in the case of bosonic atoms, and the crossover between Bose-Einstein condensation (BEC) and fermionic superfluidity described by the the theory of Bardeen, Cooper, and Schrieffer (BCS) for fermionic atoms (5). Mix-

tures of Bose-Einstein condensates were produced shortly after the observation of BEC (2), and a BEC mixed with a single-spin state Fermi sea was originally observed in (6, 7). However, realizing a mixture in which both fermionic and bosonic species are superfluid has been experimentally challenging. This has also been a long-sought goal in liquid helium, where superfluidity was achieved separately in both bosonic ^{4}He and fermionic ^{3}He. The double superfluid should undergo a transition